2

A thru-only de-embedding method for on-wafer characterization of multiport networks

Shuhei Amakawa, Noboru Ishihara, and Kazuya Masu
Tokyo Institute of Technology
Japan

1. Overview

De-embedding is the process of deducing the characteristics of a device under test (DUT) from measurements made at a distance ((Bauer & Penfield, 1974)), often via additional measurements of one or more dummy devices. This article reviews a simple thru-only de-embedding method suitable for on-wafer characterization of 2-port, 4-port, and 2n-port networks having a certain symmetry property. While most conventional de-embedding methods require two or more dummy patterns, the thru-only method requires only one THRU pattern.

If the device under measurement is a 2-port and the corresponding THRU pattern has the left/right reflection symmetry, the THRU can be mathematically split into symmetric halves and the scattering matrix for each of them can be determined (Ito & Masu, 2008; Laney, 2003; Nan et al., 2007; Song et al., 2001; Tretiakov et al., 2004a). Once those scattering matrices are available, the effects of pads and leads can be canceled and the characteristics of the device obtained. The method was applied up to 110GHz for characterization of an on-chip transmission line (TL) (Ito & Masu, 2008).

In the case of 4-port devices such as differential transmission lines, 4-port THRU patterns with ground-signal-ground-signal-ground (GSGSG) pads or GSSG pads can often be designed to have the even/odd symmetry in addition to the left/right reflection symmetry. In that case, the scattering matrix for a THRU can be transformed into a block-diagonal form representing two independent 2-ports by an even/odd transformation. Then, the 2-port thru-only de-embedding method can be applied to the resultant two 2-ports. This 4-port thru-only method was applied to de-embedding of a pair of coupled transmission lines up to 50 GHz (Amakawa et al., 2008). The result was found to be approximately consistent with that from the standard open-short method (Koolen et al., 1991), which requires two dummy patterns: OPEN and SHORT.

In the above case (Amakawa et al., 2008), the transformation matrix was known a priori because of the nominal symmetry of the THRU. However, if the 4-port THRU does not have the even/odd symmetry or if the device under measurement is a 2n-port with $n \geq 3$, the above method cannot be applied. Even if so, the thru-only method can actually be extended to 4-ports without even/odd symmetry or 2n-ports by using the recently proposed S-parameter-based modal decomposition of multiconductor transmission lines (MTLs) (Amakawa et al., 2009). A 2n-port THRU can be regarded as nonuniform multiconductor transmission lines,

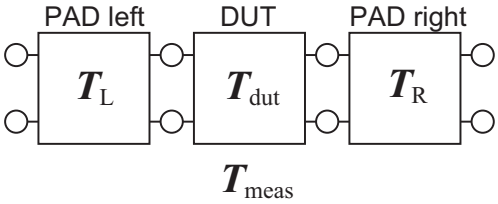

(a) A test pattern with pads and a DUT.

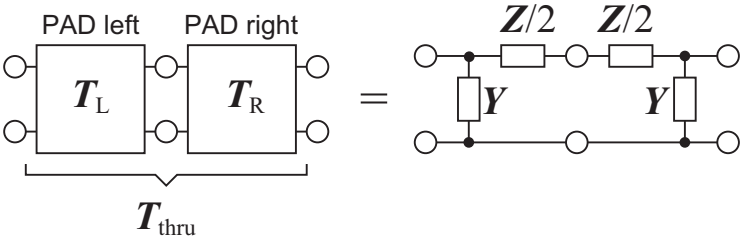

(b) Model of THRU.

Fig. 1. DUT embedded in parasitic networks.

and its scattering matrix can be transformed into a block-diagonal form with 2×2 diagonal blocks, representing n uncoupled 2-ports. The validity of the procedure was confirmed by applying it to de-embedding of four coupled transmission lines, which is an 8-port (Amakawa et al., 2009).
The thru-only de-embedding method could greatly facilitate accurate microwave and millimeter-wave characterization of on-chip multiport networks. It also has the advantage of not requiring a large area of expensive silicon real estate.

2. Introduction

Demand for accurate high-frequency characterization of on-chip devices has been escalating concurrently with the accelerated development of high-speed digital signaling systems and radio-frequency (RF) circuits. Millimeter-wave CMOS circuits have also been becoming a hot research topic.
To characterize on-chip devices and circuits, on-wafer scattering parameter (S-parameter) measurements with a vector network analyzer (VNA) have to be made. A great challenge there is how to deal with parasitics. Since an on-wafer device under test (DUT) is inevitably "embedded" in such intervening structures as probe pads and leads as schematically shown in Fig. 1(a), and they leave definite traces in the S-parameters measured by a VNA, the characteristics of the DUT have to be "de-embedded" (Bauer & Penfield, 1974) in some way from the as-measured data.
While there have been a number of de-embedding methods proposed for 2-port networks, very few have been proposed for 4-port networks in spite of the fact that many important devices, such as differential transmission lines, are represented as 4-ports. In this article, we present a simple 4-port de-embedding method that requires only a THRU pattern (Amakawa

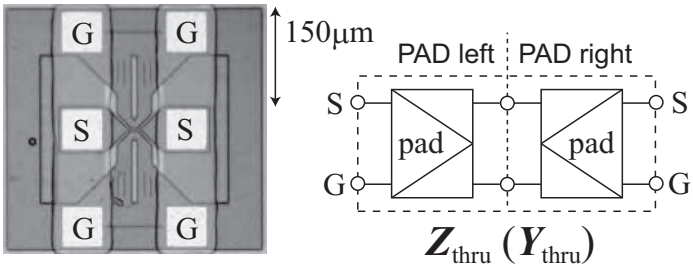

Fig. 2. Micrograph and schematic representation of THRU (Ito & Masu, 2008).

et al., 2008). This method is an extension of a thru-only method for 2-ports. In addition, we also present its extension to 2n-ports (Amakawa et al., 2009).
The rest of this article starts with a brief description of the thru-only de-embedding method for 2-ports in Section 3. It forms the basis for the multiport method. In Section 4, we explain the mode transformation theory used in the multiport de-embedding method. Section 5 presents an example of performing de-embedding by the thru-only method when the DUT is a 4-port having the even/odd symmetry. Section 6 explains how the mode transformation matrix can be found when the DUT does not have such symmetry or when the DUT is a 2n-port with $n \geq 3$. Section 7 shows examples of applying the general method. Finally, Section 8 concludes the article.

3. Thru-only de-embedding for 2-ports

Commonly used de-embedding methods usually employ OPEN and SHORT on-chip standards (dummy patterns) (Wartenberg, 2002). De-embedding procedures are becoming increasingly complex and tend to require several dummy patterns (Kolding, 2000b; Vandamme et al., 2001; Wei et al., 2007). The high cost associated with the large area required for dummy patterns is a drawback of advanced de-embedding methods.
Thru-only methods, in contrast, require only one THRU and gaining popularity (Daniel et al., 2004; Goto et al., 2008; Ito & Masu, 2008; Laney, 2003; Nan et al., 2007; Song et al., 2001; Tretiakov et al., 2004a).
In (Ito & Masu, 2008; Laney, 2003; Nan et al., 2007; Song et al., 2001; Tretiakov et al., 2004a), the THRU is modeled by a Π-type equivalent circuit shown in Fig. 1(b). The method of (Goto et al., 2008), on the other hand, was derived from (Mangan et al., 2006), which is related to (Rautio, 1991). It is applicable if the series parasitic impedance Z in Fig. 1(b) is negligible (Goto et al., 2008; Ito & Masu, 2008; Rautio, 1991). In what follows, we will focus on the method of (Ito & Masu, 2008; Laney, 2003; Nan et al., 2007; Song et al., 2001; Tretiakov et al., 2004a).
The THRU pattern used in (Ito & Masu, 2008) is shown in Fig. 2. The 150 μm-pitch ground-signal-ground (GSG) pads are connected with each other via short leads. It turned out that the THRU can be adequately represented by the frequency-independent model shown in Fig. 3. Fig. 4 shows good agreement between the measurement data and the model up to 100 GHz.
The procedure of the thru-only de-embedding method ((Ito & Masu, 2008; Laney, 2003; Nan et al., 2007; Song et al., 2001; Tretiakov et al., 2004a)) is as follows. The 2-port containing the DUT and the THRU a are assumed to be representable by Fig. 1(a) and Fig. 1(b), respectively.

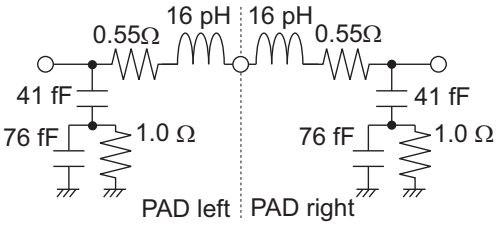

Fig. 3. Lumped-element Π-model of THRU (Ito & Masu, 2008).

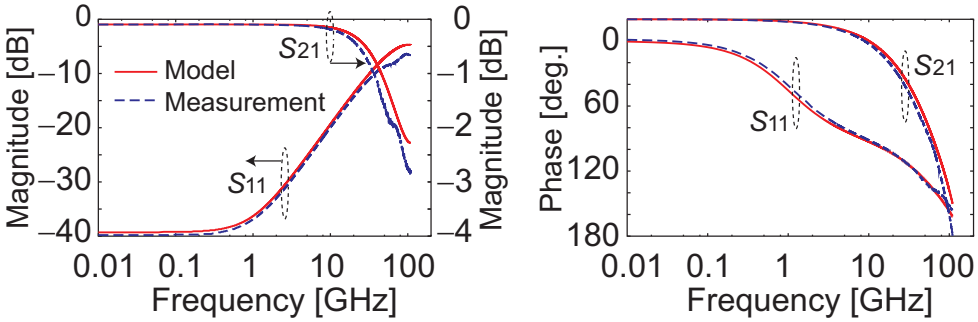

Fig. 4. Measured and modeled (Fig. 3) S-parameters of the THRU pattern. (Ito & Masu, 2008).

In terms of transfer matrices (Mavaddat, 1996), this means that

$$\mathbf{T}_{\text{meas}} = \mathbf{T}_{\text{L}}\mathbf{T}_{\text{dut}}\mathbf{T}_{\text{R}}, \tag{1}$$

$$\mathbf{T}_{\text{thru}} = \mathbf{T}_{\text{L}}\mathbf{T}_{\text{R}}. \tag{2}$$

The S-matrix and T-matrix of a 2-port are related to each other through

$$\mathbf{S} = \begin{bmatrix} S_{11} & S_{12} \\ S_{21} & S_{22} \end{bmatrix} = \frac{1}{T_{11}} \begin{bmatrix} T_{21} & \det \mathbf{T} \\ 1 & -T_{12} \end{bmatrix}, \tag{3}$$

$$\mathbf{T} = \begin{bmatrix} T_{11} & T_{12} \\ T_{21} & T_{22} \end{bmatrix} = \frac{1}{S_{21}} \begin{bmatrix} 1 & -S_{22} \\ S_{11} & -\det \mathbf{S} \end{bmatrix}. \tag{4}$$

Suppose now that the Y-matrix of the THRU is given by

$$\mathbf{Y}_{\text{thru}} = \begin{bmatrix} y_{11} & y_{12} \\ y_{12} & y_{11} \end{bmatrix}. \tag{5}$$

Note that in (5), reciprocity ($y_{21} = y_{12}$) and reflection symmetry ($y_{22} = y_{11}$) are assumed. (5) can be found by converting the measured S-matrix of the THRU into a Y-matrix through (18). If the THRU is split into symmetric halves according to the Π-equivalent in Fig. 1(b),

$$\mathbf{Y}_{\text{L}} = \begin{bmatrix} Y + 2Z^{-1} & -2Z^{-1} \\ -2Z^{-1} & 2Z^{-1} \end{bmatrix} \tag{6}$$

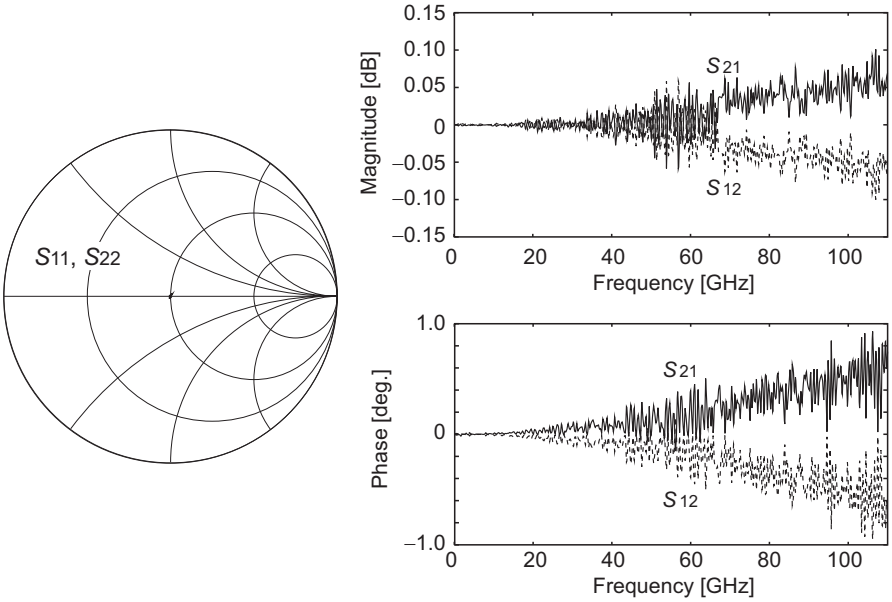

Fig. 5. De-embedded results of the THRU pattern. The thru-only de-embedding method is applied. The maximum magnitude of S_{11} is -33.7 dB (Ito & Masu, 2008).

and

$$\mathbf{Y}_{\mathrm{R}} = \begin{bmatrix} 2Z^{-1} & -2Z^{-1} \\ -2Z^{-1} & Y + 2Z^{-1} \end{bmatrix}, \tag{7}$$

respectively. The parameters in Fig. 1(b) are then given by

$$Y = y_{11} + y_{12}, \tag{8}$$

$$Z = -1/y_{12}. \tag{9}$$

The characteristics of the DUT can be de-embedded as

$$\mathbf{T}_{\mathrm{dut}} = \mathbf{T}_{\mathrm{L}}^{-1}\mathbf{T}_{\mathrm{meas}}\mathbf{T}_{\mathrm{R}}^{-1}. \tag{10}$$

For the procedure to be valid, it is necessary, at least, that the de-embedded THRU that does nothing. That is, S_{11} and S_{22} should be at the center of the Smith chart, and S_{12} and S_{21} are at (1,0). Fig. 5 shows that those do hold approximately. Published papers indicate reasonable success of the thru-only de-embedding method for 2-ports (Ito & Masu, 2008; Laney, 2003; Nan et al., 2007; Song et al., 2001; Tretiakov et al., 2004a).

4. Theory of mode transformation

4.1 General theory

In this section, we explain the theory of S-matrix mode transformation (Amakawa et al., 2008) in preparation for developing thru-only de-embedding for multiports based on the 2-port method explained in the preceding section.

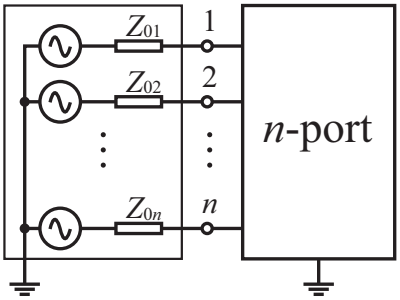

Fig. 6. The right n-port is the network under measurement. The left one is the terminating network, possibly representing a measurement system like a VNA.

A generalized scattering matrix $\mathbf{S}$ of an n-port (Fig. 6) relates the vector, $\mathbf{a}$, of power waves of a given frequency incident upon the n-port to the vector, $\mathbf{b}$, of outgoing power waves (Kurokawa, 1965; Mavaddat, 1996).

$$\mathbf{b} = \mathbf{S}\mathbf{a}, \tag{11}$$

$$\mathbf{a} = \mathbf{R}_0^{-1/2}\mathbf{v}^+ = \frac{1}{2}\mathbf{R}_0^{-1/2}(\mathbf{v} + \mathbf{Z}_0\mathbf{i}), \tag{12}$$

$$\mathbf{b} = \mathbf{R}_0^{-1/2}\mathbf{v}^- = \frac{1}{2}\mathbf{R}_0^{-1/2}(\mathbf{v} - \mathbf{Z}_0^*\mathbf{i}), \tag{13}$$

$$\mathbf{v} = \mathbf{v}^+ + \mathbf{v}^- = \mathbf{Z}\mathbf{i}, \tag{14}$$

$$\mathbf{i} = \mathbf{i}^+ + \mathbf{i}^- = \mathbf{Y}\mathbf{v}. \tag{15}$$

In (12) and (13), * denotes complex conjugate. $\mathbf{Z}_0$ is the reference impedance matrix used to define the generalized S-matrix, and $\mathbf{R}_0 = \Re(\mathbf{Z}_0)$. $\mathbf{Z}_0$ is a diagonal matrix in the conductor domain, in which actual measurements are made with a vector network analyzer (VNA). The kth diagonal element of $\mathbf{Z}_0$ is the reference impedance of the kth port. $\mathbf{Z}_0$ is usually set by a VNA to be a real scalar matrix: $\mathbf{Z}_0 = \mathbf{R}_0 = R_0\mathbf{1}_n$ with $R_0 = 50\,\Omega$. Here $\mathbf{1}_n$ is an $n \times n$ identity matrix. $\mathbf{v}$ and $\mathbf{i}$ in (14) and (15) are, respectively, the port voltage vector and the port current vector in the conductor domain. $\mathbf{Z}$ in (14) is the open-circuit impedance matrix of the n-port under measurement and its inverse is the short-circuit admittance matrix $\mathbf{Y}$ in (15). From (11) and (12), $\mathbf{S}$ and $\mathbf{Z}$ $(= \mathbf{Y}^{-1})$ can be converted to each other by

$$\mathbf{S} = \mathbf{R}_0^{-1/2}\left(\mathbf{Z} - \mathbf{Z}_0^*\right)\left(\mathbf{Z} + \mathbf{Z}_0\right)^{-1}\mathbf{R}_0^{1/2}, \tag{16}$$

$$\mathbf{Z} = \mathbf{R}_0^{1/2}\left(\mathbf{1}_2 - \mathbf{S}\right)^{-1}\left(\mathbf{R}_0^{-1/2}\mathbf{Z}_0^* + \mathbf{S}\mathbf{R}_0^{-1/2}\mathbf{Z}_0\right), \tag{17}$$

$$\mathbf{Y} = \left(\mathbf{R}_0^{-1/2}\mathbf{Z}_0^* + \mathbf{S}\mathbf{R}_0^{-1/2}\mathbf{Z}_0\right)^{-1}\left(\mathbf{1}_2 - \mathbf{S}\right)\mathbf{R}_0^{-1/2}. \tag{18}$$

A network matrix of an n-port (Fig. 6) can be transformed into a different representation by changing the basis sets for voltage and current by the following pair of transformations (Paul, 2008).

$$\mathbf{v} = \mathbf{K}_\mathrm{V}\tilde{\mathbf{v}}, \tag{19}$$

$$\mathbf{i} = \mathbf{K}_\mathrm{I}\tilde{\mathbf{i}}, \tag{20}$$

subject to

$$\mathbf{K}_{\mathrm{V}}^{\mathrm{T}}\mathbf{K}_{\mathrm{I}}^{*} = \mathbf{1}_n. \tag{21}$$

Here $^{\mathrm{T}}$ denotes matrix transposition. $\tilde{\mathbf{v}}$ and $\tilde{\mathbf{i}}$ are, respectively, the port voltage vector and the port current vector in the modal domain. (21) ensures that the power flux remains invariant under the change of bases (Paul, 2008); for example, $\mathbf{a}^{\mathrm{T}}\mathbf{a}^{*} = \tilde{\mathbf{a}}^{\mathrm{T}}\tilde{\mathbf{a}}^{*}$. (19) and (20) suggest that $\mathbf{K}_{\mathrm{V}}$ and $\mathbf{K}_{\mathrm{I}}$ can be expressed in terms of a unitary matrix $\mathbf{K}_{\mathrm{U}}$ ($\mathbf{K}_{\mathrm{U}}^{\dagger} = \mathbf{K}_{\mathrm{U}}^{-1}$) and a Hermitian matrix $\mathbf{K}_{\mathrm{P}}$ ($\mathbf{K}_{\mathrm{P}}^{\dagger} = \mathbf{K}_{\mathrm{P}}$) by polar decomposition as

$$\mathbf{K}_{\mathrm{V}} = \mathbf{K}_{\mathrm{U}}\mathbf{K}_{\mathrm{P}}, \quad \mathbf{K}_{\mathrm{I}} = \mathbf{K}_{\mathrm{U}}\mathbf{K}_{\mathrm{P}}^{-1}. \tag{22}$$

Here † denotes conjugate transpose. Since $\mathbf{v}$ and $\mathbf{i}$ are related by the Z-matrix as $\mathbf{v} = \mathbf{Z}\mathbf{i}$, impedance matrices undergo the following transformation by the change of bases (19) and (20):

$$\tilde{\mathbf{Z}} = \mathbf{K}_{\mathrm{V}}^{-1}\mathbf{Z}\mathbf{K}_{\mathrm{I}} = \mathbf{K}_{\mathrm{P}}^{-1}\mathbf{K}_{\mathrm{U}}^{\dagger}\mathbf{Z}\mathbf{K}_{\mathrm{U}}\mathbf{K}_{\mathrm{P}}^{-1}. \tag{23}$$

Likewise,

$$\tilde{\mathbf{Y}} = \mathbf{K}_{\mathrm{I}}^{-1}\mathbf{Y}\mathbf{K}_{\mathrm{V}} = \mathbf{K}_{\mathrm{P}}\mathbf{K}_{\mathrm{U}}^{\dagger}\mathbf{Y}\mathbf{K}_{\mathrm{U}}\mathbf{K}_{\mathrm{P}}. \tag{24}$$

The reference impedance matrix $\mathbf{Z}_0$ is, in fact, the impedance matrix of the terminating n-port shown in Fig. 6 (with all the signal sources shunted) and is also transformed by (23). If $\mathbf{Z}_0$ is a scalar matrix as is usually the case in the conductor domain,

$$\tilde{\mathbf{Z}}_0 = \mathbf{K}_{\mathrm{P}}^{-1}\mathbf{Z}_0\mathbf{K}_{\mathrm{P}}^{-1}. \tag{25}$$

It is only $\mathbf{K}_{\mathrm{P}}$ (and not $\mathbf{K}_{\mathrm{U}}$) that affects reference impedances.
If $\mathbf{Z}_0$ is a real scalar matrix, it can be shown that S-matrices undergo the following unitary transformation regardless of the value of $\mathbf{K}_{\mathrm{P}}$:

$$\tilde{\mathbf{S}} = \mathbf{K}_{\mathrm{U}}^{\dagger}\mathbf{S}\mathbf{K}_{\mathrm{U}}. \tag{26}$$

Mode transformation is particularly useful if the form of $\tilde{\mathbf{S}}$ is diagonal or block-diagonal because it means that the n-port is decoupled into some independent subnetworks. In some cases, the values of $\mathbf{K}_{\mathrm{V}}$ and $\mathbf{K}_{\mathrm{I}}$ that give the desired form of $\tilde{\mathbf{S}}$ might be known a priori. Mode transformation is also useful if two or more ports of a network are meant to be excited in a correlated fashion. An example includes differential circuits. In the following, we present a couple of transformations that are used often.

4.2 Even/odd transformation

We define the 2-port even/odd transformation by

$$\mathbf{v} = \begin{bmatrix} V_1 \\ V_2 \end{bmatrix} = \mathbf{K}_{\mathrm{Ve/o}}\mathbf{v}_{\mathrm{e/o}}, \tag{27}$$

$$\mathbf{i} = \begin{bmatrix} I_1 \\ I_2 \end{bmatrix} = \mathbf{K}_{\mathrm{Ie/o}}\mathbf{i}_{\mathrm{e/o}}, \tag{28}$$

$$\mathbf{K}_{\mathrm{Ve/o}} = \mathbf{K}_{\mathrm{Ie/o}} = \frac{1}{\sqrt{2}}\begin{bmatrix} 1 & 0 \\ 0 & -1 \end{bmatrix}, \tag{29}$$

$$\mathbf{v}_{\mathrm{e/o}} = \begin{bmatrix} V_{\mathrm{e}} \\ V_{\mathrm{o}} \end{bmatrix} = \frac{1}{\sqrt{2}}\begin{bmatrix} V_1 + V_2 \\ V_1 - V_2 \end{bmatrix}, \tag{30}$$

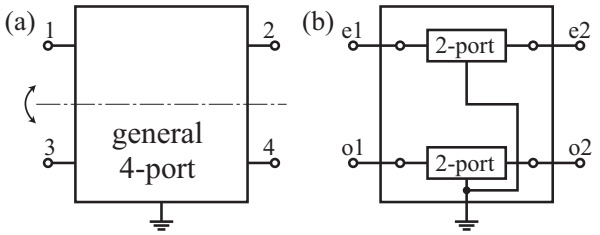

Fig. 7. (a) General 4-port. (b) 4-port consisting of a pair of uncoupled 2-ports.

$$\mathbf{i}_{\mathrm{e/o}} = \begin{bmatrix} I_{\mathrm{e}} \\ I_{\mathrm{o}} \end{bmatrix} = \frac{1}{\sqrt{2}} \begin{bmatrix} I_1 + I_2 \\ I_1 - I_2 \end{bmatrix}. \tag{31}$$

Note that $\mathbf{K}_{\mathrm{Ve/o}}$ is orthogonal ($\mathbf{K}_{\mathrm{Ve/o}}^{\mathrm{T}} = \mathbf{K}_{\mathrm{Ve/o}}^{-1}$) and, therefore,

$$\mathbf{K}_{\mathrm{U}} = \mathbf{K}_{\mathrm{Ve/o}}, \quad \mathbf{K}_{\mathrm{P}} = \mathbf{1}_n. \tag{32}$$

According to (25), the reference impedance matrix in the even/odd domain is given by

$$\mathbf{Z}_{0\mathrm{e/o}} = \mathbf{Z}_0. \tag{33}$$

This invariance of the reference impedance matrix is an advantage of the even/odd transformation. This property is consistent with the even mode and the odd mode used in microwave engineering (Pozar, 2005) and transmission line theory (Bakoglu, 1990; Magnusson et al., 2001). From (26),

$$\mathbf{S}_{\mathrm{e/o}} = \mathbf{K}_{\mathrm{Ve/o}} \mathbf{S} \mathbf{K}_{\mathrm{Ve/o}} \tag{34}$$

$$= \frac{1}{2} \begin{bmatrix} S_{11} + S_{21} + S_{12} + S_{22} & S_{11} + S_{21} - S_{12} - S_{22} \\ S_{11} - S_{21} + S_{12} - S_{22} & S_{11} - S_{21} - S_{12} + S_{22} \end{bmatrix}. \tag{35}$$

Extension of the even/odd transformation to 4-ports is straightforward as follows.

$$\mathbf{v} = \begin{bmatrix} V_1 \\ V_2 \\ V_3 \\ V_4 \end{bmatrix} = \mathbf{K}_{\mathrm{Ve/o}} \mathbf{v}_{\mathrm{e/o}}, \quad \mathbf{i} = \begin{bmatrix} I_1 \\ I_2 \\ I_3 \\ I_4 \end{bmatrix} = \mathbf{K}_{\mathrm{Ie/o}} \mathbf{i}_{\mathrm{e/o}}, \tag{36}$$

$$\mathbf{K}_{\mathrm{Ve/o}} = \mathbf{K}_{\mathrm{Ie/o}} = \frac{1}{\sqrt{2}} \begin{bmatrix} 1 & 0 & 1 & 0 \\ 0 & 1 & 0 & 1 \\ 1 & 0 & -1 & 0 \\ 0 & 1 & 0 & -1 \end{bmatrix}, \tag{37}$$

$$\mathbf{v}_{\mathrm{e/o}} = \begin{bmatrix} V_{\mathrm{e1}} \\ V_{\mathrm{e2}} \\ V_{\mathrm{o1}} \\ V_{\mathrm{o2}} \end{bmatrix} = \frac{1}{\sqrt{2}} \begin{bmatrix} V_1 + V_3 \\ V_2 + V_4 \\ V_1 - V_3 \\ V_2 - V_4 \end{bmatrix}, \quad \mathbf{i}_{\mathrm{e/o}} = \begin{bmatrix} I_{\mathrm{e1}} \\ I_{\mathrm{e2}} \\ I_{\mathrm{o1}} \\ I_{\mathrm{o2}} \end{bmatrix} = \frac{1}{\sqrt{2}} \begin{bmatrix} I_1 + I_3 \\ I_2 + I_4 \\ I_1 - I_3 \\ I_2 - I_4 \end{bmatrix}. \tag{38}$$

The corresponding port numbering is shown in Fig. 7. Clearly, the exact form of $\mathbf{K}_{\mathrm{Ve/o}}$ depends on how the ports are numbered.

Let $\mathbf{S}$ be the conductor-domain 4×4 scattering matrix as measured by a VNA.

$$\mathbf{S} = \begin{bmatrix} \mathbf{S}_{11} & \mathbf{S}_{12} \\ \mathbf{S}_{21} & \mathbf{S}_{22} \end{bmatrix} = \left[\begin{array}{cc|cc} S_{11} & S_{12} & S_{13} & S_{14} \\ S_{21} & S_{22} & S_{23} & S_{24} \\ \hline S_{31} & S_{32} & S_{33} & S_{34} \\ S_{41} & S_{42} & S_{43} & S_{44} \end{array}\right]. \tag{39}$$

From (26) and (32), the S-matrix in the even/odd domain, $\mathbf{S}_{\mathrm{e/o}}$, is given by the following orthogonal transformation.

$$\mathbf{S}_{\mathrm{e/o}} = \begin{bmatrix} \mathbf{S}_{\mathrm{ee}} & \mathbf{S}_{\mathrm{eo}} \\ \mathbf{S}_{\mathrm{oe}} & \mathbf{S}_{\mathrm{oo}} \end{bmatrix} = \mathbf{K}_{\mathrm{Ve/o}} \mathbf{S} \mathbf{K}_{\mathrm{Ve/o}}, \tag{40}$$

$$\mathbf{S}_{\mathrm{ee}} = \begin{bmatrix} S_{\mathrm{e1e1}} & S_{\mathrm{e1e2}} \\ S_{\mathrm{e2e1}} & S_{\mathrm{e2e2}} \end{bmatrix} = \frac{1}{2}\left(\mathbf{S}_{11} + \mathbf{S}_{21} + \mathbf{S}_{12} + \mathbf{S}_{22}\right), \tag{41}$$

$$\mathbf{S}_{\mathrm{eo}} = \begin{bmatrix} S_{\mathrm{e1o1}} & S_{\mathrm{e1o2}} \\ S_{\mathrm{e2o1}} & S_{\mathrm{e2o2}} \end{bmatrix} = \frac{1}{2}\left(\mathbf{S}_{11} + \mathbf{S}_{21} - \mathbf{S}_{12} - \mathbf{S}_{22}\right), \tag{42}$$

$$\mathbf{S}_{\mathrm{oe}} = \begin{bmatrix} S_{\mathrm{o1e1}} & S_{\mathrm{o1e2}} \\ S_{\mathrm{o2e1}} & S_{\mathrm{o2e2}} \end{bmatrix} = \frac{1}{2}\left(\mathbf{S}_{11} - \mathbf{S}_{21} + \mathbf{S}_{12} - \mathbf{S}_{22}\right), \tag{43}$$

$$\mathbf{S}_{\mathrm{oo}} = \begin{bmatrix} S_{\mathrm{o1o1}} & S_{\mathrm{o1o2}} \\ S_{\mathrm{o2o1}} & S_{\mathrm{o2o2}} \end{bmatrix} = \frac{1}{2}\left(\mathbf{S}_{11} - \mathbf{S}_{21} - \mathbf{S}_{12} + \mathbf{S}_{22}\right). \tag{44}$$

If the 4-port in question is symmetrical about the horizontal line shown in Fig. 7(a), the off-diagonal submatrices $\mathbf{S}_{\mathrm{eo}}$ and $\mathbf{S}_{\mathrm{oe}}$ are zero, meaning that the 4-port in the even/odd domain consists of a pair of uncoupled 2-ports as shown in Fig. 7(b). The upper and the lower 2-ports are described by $\mathbf{S}_{\mathrm{ee}}$ and $\mathbf{S}_{\mathrm{oo}}$, respectively.

4.3 Common/differential transformation

We define the 2-port common/differential transformation by

$$\mathbf{v} = \begin{bmatrix} V_1 \\ V_2 \end{bmatrix} = \mathbf{K}_{\mathrm{Vc/d}} \mathbf{v}_{\mathrm{c/d}}, \tag{45}$$

$$\mathbf{i} = \begin{bmatrix} I_1 \\ I_2 \end{bmatrix} = \mathbf{K}_{\mathrm{Ic/d}} \mathbf{i}_{\mathrm{c/d}}, \tag{46}$$

$$\mathbf{K}_{\mathrm{Vc/d}} = \begin{bmatrix} 1 & 1/2 \\ 1 & -1/2 \end{bmatrix} = \mathbf{K}_{\mathrm{Ve/o}} \begin{bmatrix} \sqrt{2} & 0 \\ 0 & 1/\sqrt{2} \end{bmatrix}, \tag{47}$$

$$\mathbf{K}_{\mathrm{Ic/d}} = \left(\mathbf{K}_{\mathrm{Vc/d}}^{\dagger}\right)^{-1} = \begin{bmatrix} 1/2 & 1 \\ 1/2 & -1 \end{bmatrix} = \mathbf{K}_{\mathrm{Ie/o}} \begin{bmatrix} 1/\sqrt{2} & 0 \\ 0 & \sqrt{2} \end{bmatrix}, \tag{48}$$

$$\mathbf{v}_{\mathrm{c/d}} = \begin{bmatrix} V_{\mathrm{c}} \\ V_{\mathrm{d}} \end{bmatrix} = \begin{bmatrix} (V_1 + V_2)/2 \\ V_1 - V_2 \end{bmatrix}, \tag{49}$$

$$\mathbf{i}_{\mathrm{c/d}} = \begin{bmatrix} I_{\mathrm{c}} \\ I_{\mathrm{d}} \end{bmatrix} = \begin{bmatrix} I_1 + I_2 \\ (I_1 - I_2)/2 \end{bmatrix}. \tag{50}$$

This definition is consistent with the common mode and the differential mode in analog circuit theory (Gray et al., 2009). The differential mode gives what is interpreted as the signal in

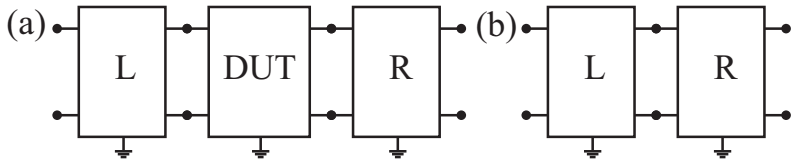

Fig. 8. (a) Model of an as-measured 4-port. The DUT is embedded in between the intervening structures L and R. (b) Model of a THRU dummy pattern.

differential circuits. The common mode describes how the pair would collectively appear when seen from far away.
Since $\mathbf{K}_{\mathrm{U}} = \mathbf{K}_{\mathrm{Ve/o}}$ and $\mathbf{K}_{\mathrm{P}} \neq \mathbf{1}_n$ as shown in (47) and (48), according to (25), $\mathbf{Z}_{0\mathrm{c/d}}$ is not equal to $\mathbf{Z}_0$. If, for example,

$$\mathbf{Z}_0 = \begin{bmatrix} 50 & 0 \\ 0 & 50 \end{bmatrix}, \tag{51}$$

then

$$\mathbf{Z}_{0\mathrm{c/d}} = \begin{bmatrix} 25 & 0 \\ 0 & 100 \end{bmatrix}. \tag{52}$$

From (26),

$$\mathbf{S}_{\mathrm{c/d}} = \mathbf{K}_{\mathrm{Ve/o}}\mathbf{S}\mathbf{K}_{\mathrm{Ve/o}} = \mathbf{S}_{\mathrm{e/o}} \tag{53}$$

$$= \frac{1}{2}\begin{bmatrix} S_{11}+S_{21}+S_{12}+S_{22} & S_{11}+S_{21}-S_{12}-S_{22} \\ S_{11}-S_{21}+S_{12}-S_{22} & S_{11}-S_{21}-S_{12}+S_{22} \end{bmatrix}. \tag{54}$$

Extension of the common/differential transformation to 4-ports is also straightforward.

$$\mathbf{v} = \mathbf{K}_{\mathrm{Vc/d}}\mathbf{v}_{\mathrm{c/d}}, \quad \mathbf{i} = \mathbf{K}_{\mathrm{Ic/d}}\mathbf{i}_{\mathrm{c/d}}, \tag{55}$$

$$\mathbf{K}_{\mathrm{Vc/d}} = \begin{bmatrix} 1 & 0 & 1/2 & 0 \\ 0 & 1 & 0 & 1/2 \\ 1 & 0 & -1/2 & 0 \\ 0 & 1 & 0 & -1/2 \end{bmatrix} = \mathbf{K}_{\mathrm{Ve/o}} \begin{bmatrix} \sqrt{2} & 0 & 0 & 0 \\ 0 & \sqrt{2} & 0 & 0 \\ 0 & 0 & 1/\sqrt{2} & 0 \\ 0 & 0 & 0 & 1/\sqrt{2} \end{bmatrix}, \tag{56}$$

$$\mathbf{K}_{\mathrm{Ic/d}} = \begin{bmatrix} 1/2 & 0 & 1 & 0 \\ 0 & 1/2 & 0 & 1 \\ 1/2 & 0 & -1 & 0 \\ 0 & 1/2 & 0 & -1 \end{bmatrix} = \mathbf{K}_{\mathrm{Ve/o}} \begin{bmatrix} 1/\sqrt{2} & 0 & 0 & 0 \\ 0 & 1/\sqrt{2} & 0 & 0 \\ 0 & 0 & \sqrt{2} & 0 \\ 0 & 0 & 0 & \sqrt{2} \end{bmatrix}, \tag{57}$$

$$\mathbf{v}_{\mathrm{c/d}} = \begin{bmatrix} V_{\mathrm{c1}} \\ V_{\mathrm{c2}} \\ V_{\mathrm{d1}} \\ V_{\mathrm{d2}} \end{bmatrix} = \begin{bmatrix} (V_1+V_3)/2 \\ (V_2+V_4)/2 \\ V_1-V_3 \\ V_2-V_4 \end{bmatrix}, \quad \mathbf{i}_{\mathrm{c/d}} = \begin{bmatrix} I_{\mathrm{c1}} \\ I_{\mathrm{c2}} \\ I_{\mathrm{d1}} \\ I_{\mathrm{d2}} \end{bmatrix} = \begin{bmatrix} I_1+I_3 \\ I_2+I_4 \\ (I_1-I_3)/2 \\ (I_2-I_4)/2 \end{bmatrix}. \tag{58}$$

$\mathbf{S}_{\mathrm{c/d}}$ is given by (53) and (40) through (44). This result is consistent with (Bockelman & Eisenstadt, 1995; Yanagawa et al, 1994) except for port ordering.

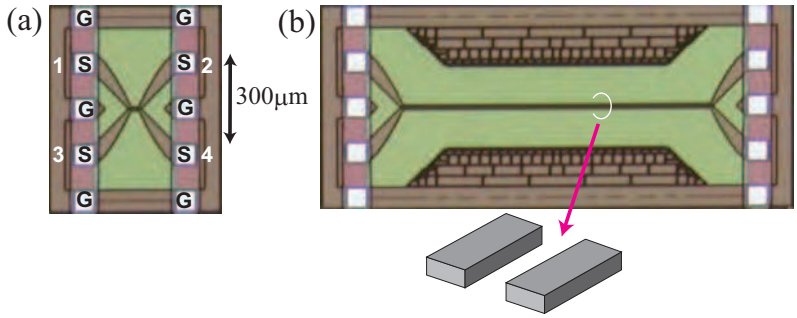

Fig. 9. (a) Micrograph of a THRU with GSGSG pads. (b) A pair of 1 mm-long TLs with the same pads. The line width is 6 μm and the spacing between the lines is 4.6 μm. Nominal differential characteristic impedance is 100 Ω. The technology is a 0.18-μm CMOS process.

5. De-embedding of 4-port with even/odd symmetry

Suppose a 4-port under measurement can be represented as a cascade of three four-ports, as shown in Fig. 8(a). Then, its transfer matrix can be written as $\mathbf{T}_{\text{meas}} = \mathbf{T}_{\text{L}}\mathbf{T}_{\text{dut}}\mathbf{T}_{\text{R}}$. As in the case of a 2-port, if the intervening structures L and R are somehow characterized, the properties of the DUT can be de-embedded by $\mathbf{T}_{\text{dut}} = \mathbf{T}_{\text{L}}^{-1}\mathbf{T}_{\text{meas}}\mathbf{T}_{\text{R}}^{-1}$. The 4-port de-embedding method proposed by (Han et al., 2003) follows this idea. Their method requires that the upper ports and the lower ports of both L and R consist of *uncoupled* two-ports as in Fig. 7(b). This condition may be fulfilled by appropriately configured off-chip systems (Han et al., 2003). However, on-chip THRU patterns (e.g. Fig. 9(a)) can hardly meet this requirement. Note, however, that an on-chip THRU, typically having GSGSG or GSSG probe pads, can often be made symmetrical about the horizontal line shown in Fig. 7(a). In that case, the S-matrix of the THRU can be decomposed into a pair of uncoupled 2-ports (Fig. 7(b)) by the even/odd transformation (40) (Amakawa et al., 2008) or, equivalently, the common/differential transformation (53). Then, each resultant 2-port can be bisected and the matrix representing each half determined as described in Section 3.

The conversion of 4-port $\mathbf{S}$ to/from $\mathbf{T}$ can be done via $\mathbf{S}'$ defined by

$$\mathbf{S}' = \begin{bmatrix} \mathbf{S}'_{11} & \mathbf{S}'_{12} \\ \mathbf{S}'_{21} & \mathbf{S}'_{22} \end{bmatrix} = \left[\begin{array}{cc|cc} S'_{11} & S'_{12} & S'_{13} & S'_{14} \\ S'_{21} & S'_{22} & S'_{23} & S'_{24} \\ \hline S'_{31} & S'_{32} & S'_{33} & S'_{34} \\ S'_{41} & S'_{42} & S'_{43} & S'_{44} \end{array}\right] = \left[\begin{array}{cc|cc} S_{11} & S_{13} & S_{12} & S_{14} \\ S_{31} & S_{33} & S_{32} & S_{34} \\ \hline S_{21} & S_{23} & S_{22} & S_{24} \\ S_{41} & S_{43} & S_{42} & S_{44} \end{array}\right], \tag{59}$$

$$\mathbf{T} = \begin{bmatrix} \mathbf{T}_{11} & \mathbf{T}_{12} \\ \mathbf{T}_{21} & \mathbf{T}_{22} \end{bmatrix} = \left[\begin{array}{cc|cc} T_{11} & T_{12} & T_{13} & T_{14} \\ T_{21} & T_{22} & T_{23} & T_{24} \\ \hline T_{31} & T_{32} & T_{33} & T_{34} \\ T_{41} & T_{42} & T_{43} & T_{44} \end{array}\right] = \begin{bmatrix} \mathbf{S}'^{-1}_{21} & -\mathbf{S}'^{-1}_{21}\mathbf{S}'_{22} \\ \mathbf{S}'_{11}\mathbf{S}'^{-1}_{21} & \mathbf{S}'_{12} - \mathbf{S}'_{11}\mathbf{S}'^{-1}_{21}\mathbf{S}'_{22} \end{bmatrix}, \tag{60}$$

$$\mathbf{S}' = \begin{bmatrix} \mathbf{T}_{21}\mathbf{T}_{11}^{-1} & \mathbf{T}_{22} - \mathbf{T}_{21}\mathbf{T}_{11}^{-1}\mathbf{T}_{12} \\ \mathbf{T}_{11}^{-1} & -\mathbf{T}_{11}^{-1}\mathbf{T}_{12} \end{bmatrix}. \tag{61}$$

We applied the proposed de-embedding method to samples fabricated with a 0.18 μm CMOS process. The frequency ranged from 100 MHz to 50 GHz. The two-step open-short method (Koolen et al., 1991) originally proposed for a two-port was also applied for comparison.

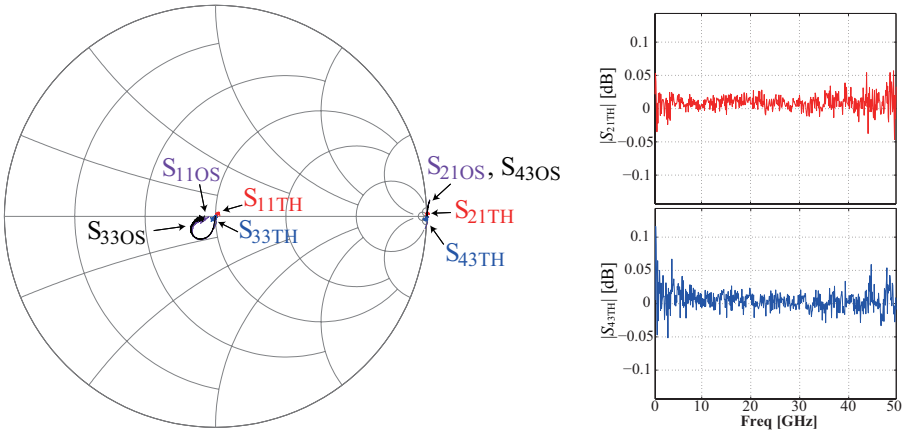

Fig. 10. Characteristics of the THRU (Fig. 9a) after performing the thru-only (S_{11TH}, S_{33TH}, S_{21TH}, S_{43TH}) or open-short (S_{11OS}, S_{33OS}, S_{21OS}, S_{43OS}) de-embedding (Amakawa et al., 2008).

Fig. 10 shows the de-embedded characteristics of a symmetric THRU itself (Fig. 9a). The reflection coefficients obtained by the proposed method (S_{11TH} and S_{33TH}) stay very close to the center of the Smith chart and the transmission coefficients (S_{21TH} and S_{43TH}) at its right end as they should. Fig. 11 shows even- and odd-mode transmission coefficients for a pair of 1 mm-long transmission lines shown in Fig. 9(b). A comparatively large difference is seen between the results from the two de-embedding methods for the even mode. One likely cause is the nonideal behavior of the SHORT (Goto et al., 2008; Ito & Masu, 2008). The odd-mode results, on the other hand, agree very well, indicating the immunity of this mode (and the differential mode) to the problem that plague the even mode (and the common mode).

6. Decomposition of a $2n$-port into n 2-ports

The essential used idea in the previous section was to reduce a 4-port problem to two independent 2-port problems by mode transformation. The requirement for it to work was that the 4×4 S matrix of the THRU dummy pattern (a pair of nonuniform TLs) have the even/odd symmetry and left/right symmetry. This development naturally leads to the idea that the same de-embedding method should be applicable to $2n$-ports, where n is a positive integer, provided that the S-matrix of the THRU (n coupled nonuniform TLs) can somehow be block-diagonalized with 2×2 diagonal blocks (Amakawa et al., 2009).

Modal analysis of multiconductor transmission lines (MTLs) have been a subject of intensive study for decades (Faria, 2004; Kogo, 1960; Paul, 2008; Williams et al., 1997). MTL equations are typically written in terms of per-unit-length equivalent-circuit parameters. Experimental characterization of MTLs, therefore, often involves extraction of those parameters from measured S-matrices (Nickel et al., 2001; van der Merwe et al., 1998). We instead directly work with S-matrices. In Section 5, the transformation matrix (37) was known a priori thanks to the even/odd symmetry of the DUT. We now have to find the transformation matrices. As before, we assume throughout that the THRU is reciprocal and hence the associated S-matrix symmetric.

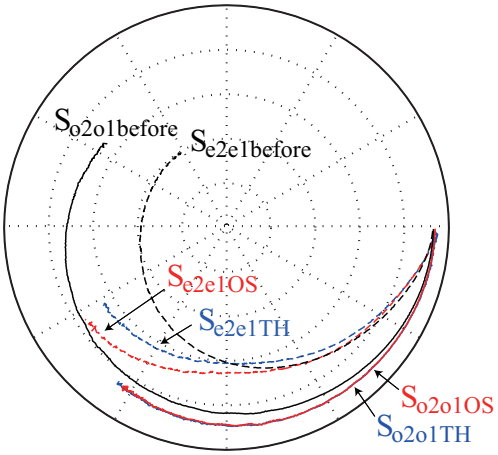

Fig. 11. Even-mode (broken lines) and odd-mode (solid lines) transmission coefficients for a pair of transmission lines (Fig. 9b) before and after de-embedding (thru-only or open-short) (Amakawa et al., 2008).

Our goal is to transform a $2n \times 2n$ scattering matrix $\mathbf{S}$ into the following block-diagonal form:

$$\tilde{\mathbf{S}}' = \begin{bmatrix} \mathbf{S}_{\mathrm{m}1} & & \\ & \ddots & \\ & & \mathbf{S}_{\mathrm{m}n} \end{bmatrix}, \tag{62}$$

where $\mathbf{S}_{\mathrm{m}i}$ are 2×2 submatrices, and the rest of the elements of $\tilde{\mathbf{S}}'$ are all 0. The port numbering for $\tilde{\mathbf{S}}'$ is shown in Fig. 12 with primes. Note that the port numbering convention adopted in this and the next Sections is different from that adopted in earlier Sections. Once the transformation is performed, the DUT can be treated as if they were composed of n uncoupled 2-ports.

This problem is not an ordinary matrix diagonalization problem. The form of (62) results by first transforming $\mathbf{S}$ into $\tilde{\mathbf{S}}$, which has the following form:

$$\tilde{\mathbf{S}} = \left[\begin{array}{c|c} \ddots & \ddots \\ \hline \ddots & \ddots \end{array}\right], \tag{63}$$

and then reordering the rows and columns of $\tilde{\mathbf{S}}$ such that $\mathbf{S}_{\mathrm{m}i}$ in (62) is built from the ith diagonal elements of the four submatrices of $\tilde{\mathbf{S}}$ (Amakawa et al., 2009). The port indices of $\tilde{\mathbf{S}}$ are shown in Fig. 12 without primes. The problem, therefore, is the transformation of $\mathbf{S}$ into $\tilde{\mathbf{S}}$ followed by reordering of rows and columns yielding $\tilde{\mathbf{S}}'$.

In the case of a cascadable $2n$-port, it makes sense to divide the ports into two groups as shown in Fig. 12, and hence the division of $\mathbf{S}$, $\mathbf{a}$, and $\mathbf{b}$ into submatrices/subvectors:

$$\mathbf{b} = \begin{bmatrix} \mathbf{b}_1 \\ \mathbf{b}_2 \end{bmatrix} = \begin{bmatrix} \mathbf{S}_{11} & \mathbf{S}_{12} \\ \mathbf{S}_{21} & \mathbf{S}_{22} \end{bmatrix} \begin{bmatrix} \mathbf{a}_1 \\ \mathbf{a}_2 \end{bmatrix} = \mathbf{S}\mathbf{a}. \tag{64}$$

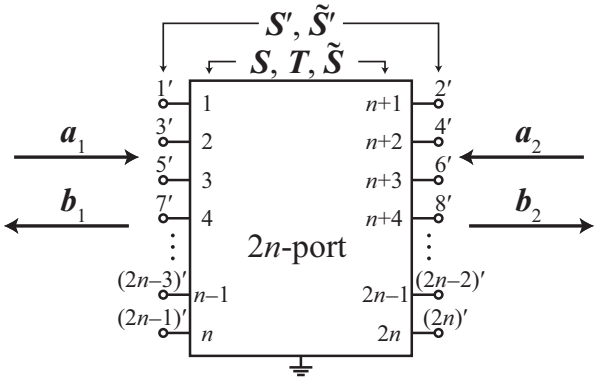

Fig. 12. Port indices for a cascadable $2n$-port. The ports 1 through n of $\mathbf{S}$ constitute one end of the bundle of n lines and the ports $n+1$ through $2n$ the other end.

This was already done in earlier Sections for 4-ports. Since our $2n$-port is reciprocal by assumption, $\mathbf{S}$ is symmetric: $\mathbf{S}^{\mathrm{T}} = \mathbf{S}$. Then, it can be shown that the following change of bases gives the desired transformation.

$$\begin{bmatrix} \mathbf{a}_1 \\ \mathbf{a}_2 \end{bmatrix} = \begin{bmatrix} \mathbf{W}_1 & \\ & (\mathbf{W}_2^{\mathrm{T}})^{-1} \end{bmatrix} \begin{bmatrix} \tilde{\mathbf{a}_1} \\ \tilde{\mathbf{a}_2} \end{bmatrix}, \tag{65}$$

$$\begin{bmatrix} \mathbf{b}_1 \\ \mathbf{b}_2 \end{bmatrix} = \begin{bmatrix} (\mathbf{W}_1^{\mathrm{T}})^{-1} & \\ & \mathbf{W}_2 \end{bmatrix} \begin{bmatrix} \tilde{\mathbf{b}_1} \\ \tilde{\mathbf{b}_2} \end{bmatrix}, \tag{66}$$

where the blanks represent zero submatrices. $\mathbf{W}_1$ and $\mathbf{W}_2$ diagonalize $\mathbf{S}_{21}^{-1}\mathbf{S}_{22}\mathbf{S}_{12}^{-1}\mathbf{S}_{11}$ and $\mathbf{S}_{22}\mathbf{S}_{12}^{-1}\mathbf{S}_{11}\mathbf{S}_{21}^{-1}$, respectively, by similarity transformation:

$$\mathbf{W}_1^{-1}\mathbf{S}_{21}^{-1}\mathbf{S}_{22}\mathbf{S}_{12}^{-1}\mathbf{S}_{11}\mathbf{W}_1 = \mathbf{\Lambda}_1, \tag{67}$$

$$\mathbf{W}_2^{-1}\mathbf{S}_{22}\mathbf{S}_{12}^{-1}\mathbf{S}_{11}\mathbf{S}_{21}^{-1}\mathbf{W}_2 = \mathbf{\Lambda}_2, \tag{68}$$

where $\mathbf{\Lambda}_1$ and $\mathbf{\Lambda}_2$ are diagonal matrices. $\mathbf{W}_1$ and $\mathbf{W}_2$ can be computed by eigenvalue decomposition. The derivation is similar to (Faria, 2004). $\tilde{\mathbf{S}}$ is thus given by

$$\tilde{\mathbf{S}} = \begin{bmatrix} \mathbf{W}_1^{\mathrm{T}}\mathbf{S}_{11}\mathbf{W}_1 & \mathbf{W}_1^{\mathrm{T}}\mathbf{S}_{12}(\mathbf{W}_2^{\mathrm{T}})^{-1} \\ \mathbf{W}_2^{-1}\mathbf{S}_{21}\mathbf{W}_1 & \mathbf{W}_2^{-1}\mathbf{S}_{22}(\mathbf{W}_2^{\mathrm{T}})^{-1} \end{bmatrix}. \tag{69}$$

7. Multiport de-embedding using a THRU

Suppose, as before, that the device under measurement and the THRU can be represented as shown in Fig. 13. Here the DUT is MTLs. In terms of the transfer matrix $\mathbf{T}$ defined by

$$\begin{bmatrix} \mathbf{a}_1 \\ \mathbf{b}_1 \end{bmatrix} = \mathbf{T} \begin{bmatrix} \mathbf{b}_2 \\ \mathbf{a}_2 \end{bmatrix} = \begin{bmatrix} \mathbf{T}_{11} & \mathbf{T}_{12} \\ \mathbf{T}_{21} & \mathbf{T}_{22} \end{bmatrix} \begin{bmatrix} \mathbf{b}_2 \\ \mathbf{a}_2 \end{bmatrix}, \tag{70}$$

$$\mathbf{T} = \begin{bmatrix} \mathbf{T}_{11} & \mathbf{T}_{12} \\ \mathbf{T}_{21} & \mathbf{T}_{22} \end{bmatrix} = \begin{bmatrix} \mathbf{S}_{21}^{-1} & -\mathbf{S}_{21}^{-1}\mathbf{S}_{22} \\ \mathbf{S}_{11}\mathbf{S}_{21}^{-1} & \mathbf{S}_{12} - \mathbf{S}_{11}\mathbf{S}_{21}^{-1}\mathbf{S}_{22} \end{bmatrix}, \tag{71}$$

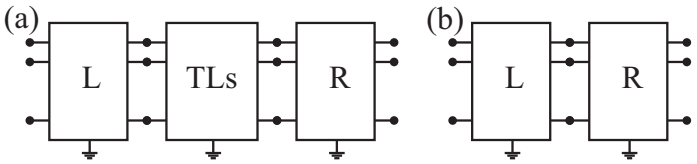

Fig. 13. (a) Model of n coupled TLs measured by a VNA. The TLs sit between the intervening structures L and R. (b) Model of a THRU.

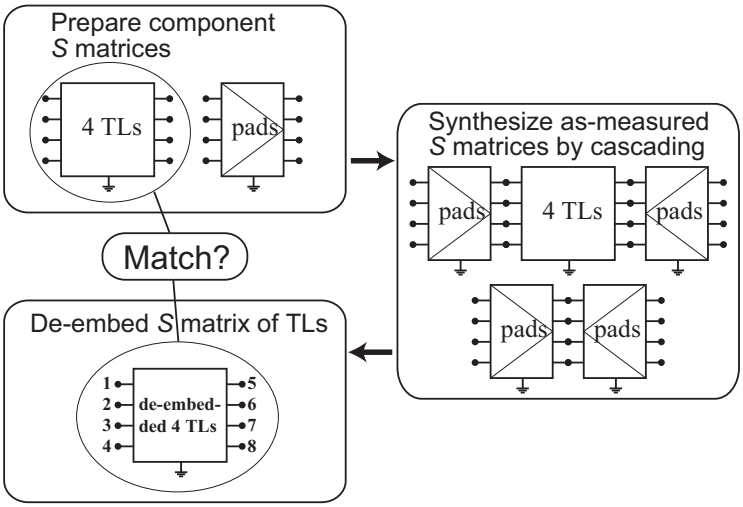

Fig. 14. Flow of validating the de-embedding method.

$$\mathbf{S} = \begin{bmatrix} \mathbf{S}_{11} & \mathbf{S}_{12} \\ \mathbf{S}_{21} & \mathbf{S}_{22} \end{bmatrix} = \begin{bmatrix} \mathbf{T}_{21}\mathbf{T}_{11}^{-1} & \mathbf{T}_{22} - \mathbf{T}_{21}\mathbf{T}_{11}^{-1}\mathbf{T}_{12} \\ \mathbf{T}_{11}^{-1} & -\mathbf{T}_{11}^{-1}\mathbf{T}_{12} \end{bmatrix}. \tag{72}$$

The as-measured T-matrix for Fig. 13(a) is $\mathbf{T}_{\text{meas}} = \mathbf{T}_{\text{L}}\mathbf{T}_{\text{TL}}\mathbf{T}_{\text{R}}$.

In order to de-embed $\mathbf{T}_{\text{TL}}$ from $\mathbf{T}_{\text{meas}}$, the THRU (Fig. 13(b)) is measured, and the result ($\mathbf{T}_{\text{thru}} = \mathbf{T}_{\text{L}}\mathbf{T}_{\text{R}}$) is transformed into the block-diagonal form $\tilde{\mathbf{S}}'_{\text{thru}}$. Since each of the resultant 2×2 diagonal blocks of $\tilde{\mathbf{S}}'_{\text{thru}}$ is symmetric by assumption, the method in Section 3 can be applied to determine $\mathbf{T}_{\text{L}}$ and $\mathbf{T}_{\text{R}}$. Then, the characteristics of the TLs are obtained by $\mathbf{T}_{\text{TL}} = \mathbf{T}_{\text{L}}^{-1}\mathbf{T}_{\text{meas}}\mathbf{T}_{\text{R}}^{-1}$.

Shown in Fig. 14 is the procedure that we followed to validate the thru-only de-embedding method for $2n$-ports (Amakawa et al., 2009). S-parameter files of 1 mm-long 4 coupled TLs and pads were generated by using Agilent Technologies ADS. A cross section of the TLs is shown in Fig. 15. The schematic diagram representing the pads placed at each end of the bundle of TLs is shown in Fig. 16. Figs. 17 and 18 show the characteristics of the "as-measured" TLs and the THRU, respectively. The characteristics of the bare (un-embedded) TLs and the de-embedded results are both shown on the same Smith chart in Fig. 19, but they are indistinguishable, thereby demonstrating the validity of the de-embedding procedure.

We also applied the same de-embedding method to the TLs shown in Fig. 9, analyzed earlier by the even/odd transformation in Section 5 (Amakawa et al., 2008). The numerical values

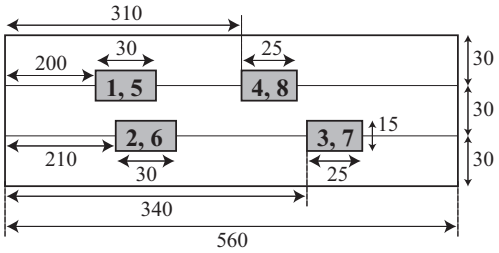

Fig. 15. Schematic cross section of the 1 mm-long 4 coupled TLs (not to scale), labeled with port numbers. Dimensions are in μm. Relative dielectric permittivity is 4. Metal conductivity is $5.9 \times 10^7\ (\Omega \cdot \mathrm{m})^{-1}$. $\tan\delta = 0.04$ (Amakawa et al., 2009).

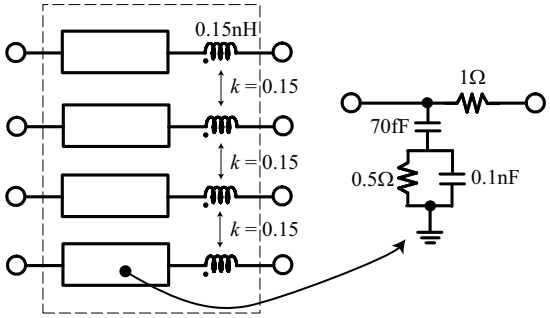

Fig. 16. Model of the left half of the THRU including pads (Amakawa et al., 2009).

of even/odd transformed and fully block-diagonalized S-matrix of the THRU (Fig. 9(a)) at 10 GHz are, respectively,

$$\mathbf{S}'_{\mathrm{e/o}} = \begin{bmatrix} 0.050-0.064\mathrm{j} & 0.828-0.369\mathrm{j} & 0.001-0.000\mathrm{j} & 0.001-0.000\mathrm{j} \\ 0.828-0.369\mathrm{j} & 0.051-0.064\mathrm{j} & -0.000+0.002\mathrm{j} & 0.001+0.000\mathrm{j} \\ 0.001-0.000\mathrm{j} & -0.000+0.002\mathrm{j} & -0.030-0.124\mathrm{j} & 0.904-0.322\mathrm{j} \\ 0.001-0.000\mathrm{j} & 0.001+0.000\mathrm{j} & 0.904-0.322\mathrm{j} & -0.030-0.123\mathrm{j} \end{bmatrix},$$

$$\tilde{\mathbf{S}}' = \begin{bmatrix} 0.051-0.064\mathrm{j} & 0.828-0.369\mathrm{j} & 0.000+0.000\mathrm{j} & 0.000+0.000\mathrm{j} \\ 0.828-0.369\mathrm{j} & 0.050-0.064\mathrm{j} & 0.000+0.000\mathrm{j} & 0.000+0.000\mathrm{j} \\ 0.000+0.000\mathrm{j} & 0.000+0.000\mathrm{j} & -0.030-0.124\mathrm{j} & 0.903-0.324\mathrm{j} \\ 0.000+0.000\mathrm{j} & 0.000+0.000\mathrm{j} & 0.903-0.324\mathrm{j} & -0.032-0.123\mathrm{j} \end{bmatrix}.$$

The reference impedance matrices are $\mathbf{Z}'_{0\mathrm{e/o}} = \tilde{\mathbf{Z}}'_0 = 50 \cdot \mathbf{1}_4$. The upper diagonal block in $\mathbf{S}'_{\mathrm{e/o}}$ is the even-mode S matrix and the lower diagonal block is the odd-mode S matrix. The residual nonzero off-diagonal blocks in $\mathbf{S}'_{\mathrm{e/o}}$, representing the crosstalk between the even and odd modes, were ignored in Section 5 (Amakawa et al., 2008). The transformation (69) can better block-diagonalize the S-matrix.

8. Conclusions

We have reviewed the simple thru-only de-embedding method for characterizing multiport networks at GHz frequencies. It is based on decomposition of a $2n$-port into n uncoupled

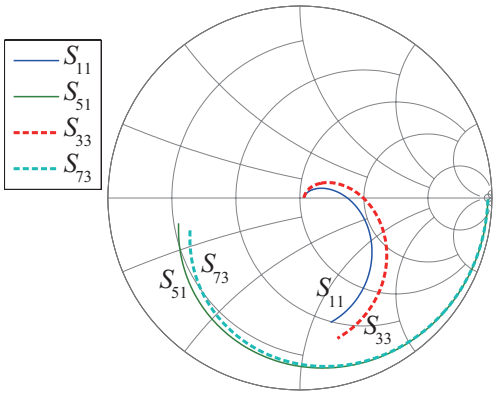

Fig. 17. Characteristics of the 4 coupled TLs from 100 MHz to 40 GHz before de-embedding (Amakawa et al., 2009).

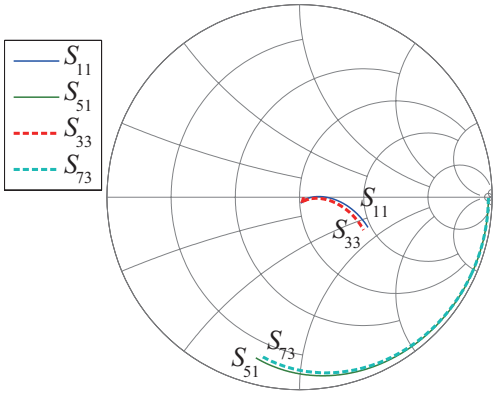

Fig. 18. Characteristics of the THRU from 100 MHz to 40 GHz (Amakawa et al., 2009).

2-ports. After the decomposition, the 2-port thru-only de-embedding method is applied. If the DUT is a 4-port and the THRU pattern has the even/odd symmetry, the transformation matrix is simple and known a priori (Amakawa et al., 2008). If not, the S-parameter-based decomposition proposed in (Amakawa et al., 2009) can be used.

While the experimental results reported so far are encouraging, the validity and applicability of the de-embedding method should be assessed carefully. It is extremely important to ascertain the validity of the 2-port de-embedding method because the validity of the multiport method depends entirely on it. One Fig. 1(b) In particular, hardly any justification has been given for the validity of the Π-equivalent-based bisecting of the THRU (Ito & Masu, 2008; Laney, 2003; Nan et al., 2007; Song et al., 2001; Tretiakov et al., 2004a). There are other possible ways of bisecting the THRU. T-equivalent-based bisection is one example (Kobrinsky et al., 2005). Once the foundations of the 2-port method are more firmly established, the multiport method can be used with greater confidence.

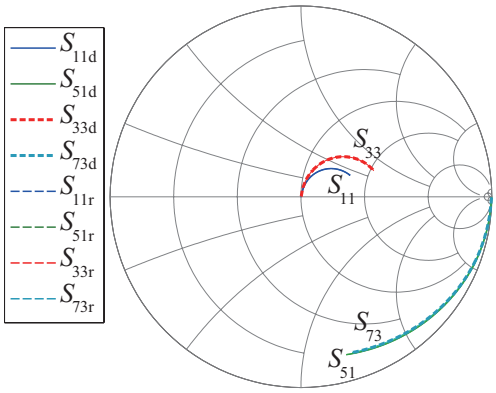

Fig. 19. Reference characteristics of the 4 coupled TLs (with a subscript r) and the de-embedded results. (with a subscript d). Actually, those two are indistinguishable on the Smith chart (Amakawa et al., 2009).

9. Acknowledgments

The authors thank H. Ito, T. Sato, T. Sekiguchi, and K. Yamanaga for useful discussions. This work was partially supported by KAKENHI, MIC.SCOPE, STARC, Special Coordination Funds for Promoting Science and Technology, and VDEC in collaboration with Agilent Technologies Japan, Ltd., Cadence Design Systems, Inc., and Mentor Graphics, Inc.

10. References

Amakawa, S., Ito, H., Ishihara, N., and Masu, K. (2008). A simple de-embedding method for characterization of on-chip four-port networks, *Advanced Metallization Conference*, pp. 105–106; *Proceedings of Advanced Metallization Conference 2008 (AMC 2008)*, pp. 99–103, 2009, Materials Research Society.

Amakawa, S., Yamanaga, K., Ito, H., Sato, T., Ishihara, N., and Masu, K. (2009). *S*-parameter-based modal decomposition of multiconductor transmission lines and its application to de-embedding, *International Conference on Microelectronic Test Structures*, pp. 177–180.

Bakoglu, H. B., *Circuits, Interconnections, and Packaging for VLSI*, Addison Wesley, 1990.

Bauer, R. F. and Penfield, Jr, P. (1974). De-embedding and unterminating, *IEEE Transactions on Microwave Theory and Techniques*, vol. 22, no. 3, pp. 282–288.

Bockelman, D. E. and Eisenstadt, W. R. (1995). Combined differential and common-mode scattering parameters: theory and simulation, *IEEE Transactions on Microwave Theory and Techniques*, vol. 43, no. 7, pp. 1530–1539.

Daniel, E. S., Harff, N. E., Sokolov, V., Schreiber, S. M., and Gilbert, B. K. (2004). Network analyzer measurement de-embedding utilizing a distributed transmission matrix bisection of a single THRU structure, *63rd ARFTG Conference*, pp. 61–68.

Faria, J. A. B. (2004). A new generalized modal analysis theory for nonuniform multiconductor transmission lines, *IEEE Transactions on Power Systems*, vol. 19, no. 2, pp. 926–933.

Goto, Y., Natsukari, Y. , and Fujishima, M. (2008). New on-chip de-embedding for accurate evaluation of symmetric devices, *Japanese Journal of Applied Physics*, vol. 47, no. 4, pp. 2812–2816.

P. R. Gray, P. J. Hurst, S. H. Lewis, and R. G. Meyer, *Analysis and Design of Analog Integrated Circuits*, 5th edition, Wiley, 2009.

Han, D.-H., Ruttan, T. G., and Polka, L. A. (2003), Differential de-embedding methodology for on-board CPU socket measurements, *61st ARFTG Conference*, pp.37–43.

Issakov, V., Wojnowski, M., Thiede, A., and Maurer, L. (2009). Extension of thru de-embedding technique for asymmetrical and differential devices, *IET Circuits, Devices & Systems*, vol. 3, no. 2, pp. 91–98.

Ito, H. and Masu, K. (2008). A simple through-only de-embedding method for on-wafer S-parameter measurements up to 110 GHz, *IEEE MTT-S International Microwave Symposium*, pp. 383–386.

Kobrinsky, M. J., Chakravarty, S., Jiao, D., Harmes, M. C., List, S., and Mazumder, M. (2005). Experimental validation of crosstalk simulations for on-chip interconnects using S-parameters, *IEEE Transactions on Advanced Packaging*, vol. 28, no. 1, pp. 57–62.

Kogo, H. (1960). A study of multielement transmission lines, *IRE Transactions on Microwave Theory and Techniques*, vol. 8, no. 2, pp. 136–142.

Kolding, T. E. (1999). On-wafer calibration techniques for giga-Hertz CMOS measurements, *International Conference on Microelectronic Test Structures*, pp.105–110.

Kolding, T. E. (2000a). Impact of test-fixture forward coupling on on-wafer silicon device measurements, *IEEE Microwave Guided Wave Letters*, vol. 10, no. 2, pp. 73–74.

Kolding, T. E. (2000b). A four-step method for de-embedding gigahertz on-wafer CMOS measurements, *IEEE Transactions on Electron Devices*, vol. 47, no. 4, pp. 734–740.

Koolen, M. C. A. M., Geelen, J. A. M., and Versleijen, M. P. J. G. (1991). An improved de-embedding technique for on-wafer high-frequency characterization, *Bipolar Circuits and Technology Meeting*, pp.188–191.

Kurokawa, K. (1965). Power waves and the scattering matrix, *IEEE Transactions on Microwave Theory and Techniques*, vol. 13, no. 2, pp. 194–202.

Laney, D. C. (2003). *Modulation, Coding and RF Components for Ultra-Wideband Impulse Radio*, PhD thesis, University of California, San Diego, San Diego, California.

Magnusson, P. C., Alexander, G. C., Tripathi, V. K., and Weisshaar, A., *Transmission Lines and Wave Propagation*, 4th edition, CRC Press, 2001.

Mangan, A. M., Voinigescu, S. P., Yang, M.-T., and Tazlauanu, M. (2006). De-embedding transmission line measurements for accurate modeling of IC designs, *IEEE Transactions on Electron Devices*, vol. 53, no. 2, pp. 235–241.

Mavaddat, R. (1996). *Network Scattering Parameters*, World Scientific.

Nan, L., Mouthaan, K., Xiong, Y.-Z., Shi, J., Rustagi, S. C., and Ooi, B.-L. (2007) Experimental characterization of the effect of metal dummy fills on spiral inductors, *Radio Frequency Integrated Circuits Symposium*, pp. 307–310.

Nickel, J. G., Trainor, D., and Schutt-Ainé, J. E. (2001). Frequency-domain-coupled microstripline normal-mode parameter extraction from *S*-parameters, *IEEE Transactions on Electromagnetic Compatibility*, vol. 43, no. 4, pp. 495–503.

Paul, C. R. (2008). *Analysis of Multiconductor Transmission Lines*, 2nd edition, Wiley-Interscience.

Pozar, D. M., *Microwave Engineering*, 3rd edition, Wiley, 2005.

Rautio, J. C. (1991). A new definition of characteristic impedance, *IEEE MTT-S International Microwave Symposium*, pp. 761–764.

Song, J., Ling, F., Flynn, G., Blood, W., and Demircan, E. (2001). A de-embedding technique for interconnects, *IEEE Topical Meeting on Electrical Performance and Electronic Packaging*, pp. 129–132.

Tretiakov, Y., Vaed, K., Ahlgren, D., Rascoe, J., Venkatadri, S., and Woods, W. (2004a). On-wafer de-embedding techniques for SiGe/BiCMOS/RFCMOS transmission line interconnect characterization, *International Interconnect Technology Conference*, pp. 166–168.

van der Merwe, J., Reader, H. C., and Cloete, J. H. (1998). *S*-parameter measurements yielding the characteristic matrices of multiconductor transmission lines, *IEEE Transactions on Electromagnetic Compatibility*, vol. 40, no. 3, pp. 249–256.

Vandamme, E. P., Schreurs, D. M. M.-P., and van Dinther, C. (2001). Improved three-step de-embedding method to accurately account for the influence of pad parasitics in silicon on-wafer RF test-structures, *IEEE Transactions on Electron Devices*, vol. 48, no. 4, pp. 737–742.

Wartenberg, S. A. (2002). *RF Measurements of Die and Packages*, Artech House.

Wei, X., Niu, G., Sweeney, S. L., Liang, Q., Wang, X., and Taylor, S. S. (2007). A general 4-port solution for 110 GHz on-wafer transistor measurements with or without impedance standard substrate (ISS) calibration, *IEEE Transactions on Electron Devices*, vol. 54, no. 10, pp. 2706–2714.

Williams, D. F., Hayden, L. A., and Marks, R. B. (1997). A complete multimode equivalent-circuit theory for electrical design, *Journal of Research of the National Institute of Standards and Technology*, vol. 102, no. 4, pp. 405–423.

Yanagawa, K., Yamanaka, K., Furukawa, T., and Ishihara, A. (1994). A measurement of balanced transmission line using *S*-parameters, *IEEE Instrumentation and Measurement Technology Conference*, pp.866–869.

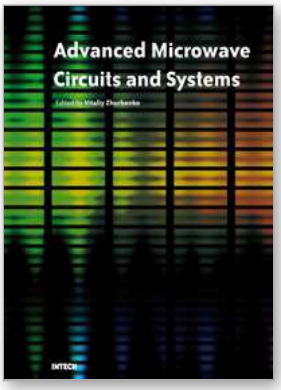

Advanced Microwave Circuits and Systems

Edited by Vitaliy Zhurbenko

ISBN 978-953-307-087-2
Hard cover, 490 pages
Publisher InTech
Published online 01, April, 2010
Published in print edition April, 2010

This book is based on recent research work conducted by the authors dealing with the design and development of active and passive microwave components, integrated circuits and systems. It is divided into seven parts. In the first part comprising the first two chapters, alternative concepts and equations for multiport network analysis and characterization are provided. A thru-only de-embedding technique for accurate on-wafer characterization is introduced. The second part of the book corresponds to the analysis and design of ultra-wideband low- noise amplifiers (LNA).

InTech Europe
University Campus STeP Ri
Slavka Krautzeka 83/A
51000 Rijeka, Croatia
Phone: +385 (51) 770 447
Fax: +385 (51) 686 166
www.intechopen.com

InTech China
Unit 405, Office Block, Hotel Equatorial Shanghai
No.65, Yan An Road (West), Shanghai, 200040, China
中国上海市延安西路65号上海国际贵都大饭店办公楼405单元
Phone: +86-21-62489820
Fax: +86-21-62489821